

Fusion of strings as a hadronic accelerator

N. Armesto, M. A. Braun*, E. G. Ferreiro, C. Pajares and Yu. M. Shabelski**

*Departamento de Física de Partículas, Universidade de Santiago de Compostela,
15706-Santiago de Compostela, Spain*

Abstract

It is shown that the fusion of strings is a source of particle production in nucleus–nucleus collisions outside the kinematical limits of nucleon–nucleon collisions. The spectrum of different particles is compared with the high energy data on p–A collisions obtaining a reasonable agreement. Results for A–B collisions at $\sqrt{s} = 19.4$ AGeV and $\sqrt{s} = 200$ AGeV are given. It is shown that the fusion of strings can accelerate particles up to the highest energy detected in cosmic rays without help of any additional cosmic accelerator. Also the rise of the average shower depth of maximum for cosmic rays in the energy range between 10^{16} eV and 10^{19} eV can be explained by the same mechanism without requiring any change in the chemical composition.

* Visiting Professor IBERDROLA. Permanent address: Department of High Energy Physics, University of St. Petersburg, 198904 St. Petersburg, Russia.

** Permanent address: Petersburg Nuclear Physics Institute, Gatchina, 188350 St. Petersburg, Russia.

1 Introduction

Several models of hadronic interactions have been very successful in describing particle production in hadron–hadron, hadron–nucleus and nucleus–nucleus collisions. Monte Carlo versions of these models are in reasonable agreement with most of the properties of soft multiparticle production. In these models ([1, 2, 3, 4]) strings, chains or pomerons are exchanged between the projectile and target. The number of strings grows with the energy and with the number of nucleons of the participant nuclei. In the first approximation strings fragment into particles and resonances in an independent way. The only correlation among strings is due to energy–momentum conservation. However, the interaction between strings becomes important with their number growing. Even at SPS energies both a large number and a large density of strings are expected. For instance, for S–S and Pb–Pb central collisions the estimated number of strings are 120 and 1300, respectively, and their densities 3.3 fm^{-2} and 9.8 fm^{-2} , respectively. At the relativistic heavy ion collider (RHIC) and large hadron collider (LHC) energies the number and density of strings are not negligibly small even for hadron–hadron collisions.

The interaction between strings or the interaction of resonances produced in the fragmentation of strings have been introduced in some of the models ([5, 6, 7, 8, 9, 10]). In particular, fusion of strings has been incorporated into the Dual Parton Model (DPM) ([8]) and the Quark Gluon String Model (QGSM) ([11]). Some of the effects of string fusion, like strangeness and antibaryon enhancement ([12]), reduction of long range correlations ([13]) and multiplicity suppression, are in reasonable agreement with the existing experimental data. Also predictions for the Relativistic Heavy Ion Collider (RHIC) and Large Hadron Collider (LHC) are available. In this paper we explore another effect of string fusion, namely particle production in nucleus–nucleus collisions

outside the kinematical limits of nucleon–nucleon collisions (the so-called cumulative effect).

It is shown that at present available energies a non negligible number of baryons and mesons are produced with momenta greater than the ones of the colliding nucleons. Essentially, the particles produced outside the kinematical limit are protons and neutrons but an appreciable number of π 's and Λ 's are also predicted. This effect, together with the reduction of multiplicities, provides a natural explanation of some features of cosmic ray data, like the rise of the average shower depth of maximum X_{max} (the amount of air penetrated by the cascade when it reaches maximum size) ([14, 15]) with increasing energy from 10^{17} eV to 10^{19} eV, and the existence of events with energy above 10^{20} eV ([14, 16, 17]), higher than the expected cut-off ([18, 19, 20]) due to the scattering of cosmic rays with the microwave radiation background. Usually the first feature is explained by an enrichment of protons in the composition of primary cosmic rays ([15]) as energy increases. However, as we shall show, if the composition of the primary cosmic rays is kept fixed in the energy range between 10^{17} eV and 10^{19} eV, string fusion leads to a suppression of the multiplicity similar to the one produced by changing heavy nuclei (Fe) by protons in the composition of the primary. On the other hand, since the momentum of a fused string is a sum of the momenta of its ancestor strings, it is possible to obtain particles with more energy than the initial nucleon–nucleon energy. As in a considerable part of events the primary would be iron, several string could fuse in central Fe–Air collisions. Therefore, the observed cosmic ray events with energy above 10^{20} eV may actually correspond to three or four times less initial energy per nucleon than the one apparently measured. Reducing the energy by a factor three, the attenuation mean free path can grow more than an order of magnitude. String fusion could make these events compatible with the existence of the above mentioned cut-off.

2 String fusion in the Monte Carlo code

To study the particle production outside the kinematical limits of nucleon–nucleon collisions we use a Monte Carlo code based on the QGSM, in which the fusion of strings has been incorporated ([11]). A detailed description of the Monte Carlo String Fusion Model (SFMC) and comparison with experimental data can be found in Refs. [11, 12, 13]. A hadron or nucleus collision is assumed to be an interaction between clouds of partons formed long before the collision. Without string fusion partons are assumed to interact only once. Each parton–parton interaction leads to the creation of colour strings. Since both the projectile and the target must remain colourless, strings have to be formed in pairs. For instance, in nucleon–nucleon collisions at moderate energies a pair of strings is formed between a valence diquark of the projectile and a valence quark of the target and between a valence quark of the projectile and a valence diquark of the target. As the energy increases, pairs of strings are also formed between sea quarks (antiquarks) of the projectile and sea antiquarks (quarks) of the target. Hadrons and nuclei are considered on the same footing. The nuclear wave function is taken as a convolution of the parton distribution in a nucleon with the distribution of nucleons in the nucleus. For the distributions of partons and nucleons we take gaussian (centered in each nucleon) and Wood–Saxon shapes respectively.

Strings fuse when their transverse positions come within a certain interaction area, which is fixed previously to describe correctly the strangeness enhancement ([12]) shown by the data on nucleus–nucleus collisions. Fusion can take place only when the rapidity intervals of the strings overlap. It is formally described by allowing partons to interact several times, the number of interactions being the same for projectile and target. The quantum numbers of the fused string are determined by those of the interacting partons and its energy–momentum is the sum of the energy–momentum of the ancestor strings.

The colour charges of the fusing string ends sum into the colour charge of the resulting string ends according to the $SU(3)$ composition laws. In particular, two triplet strings fuse into an antitriplet and a sextet string, with probabilities $1/3$ and $2/3$ respectively. A triplet and an antitriplet string give rise to a singlet state and an octet string with probabilities $1/9$ and $8/9$ respectively. In present calculations only fusion of two strings is taken into account.

A quasi-classical picture of the decay of colour strings is assumed in which pairs of oppositely colour partons are produced in the string colour field, which neutralizes this field and leads to string breaking. The new sextet and octet strings are supposed to break with the production of two (anti) quark complexes with the same colour charges Q and $-Q$ as those of the ends of the string. The created (anti) quarks have arbitrary flavours and masses chosen as the corresponding constituent masses. The probability rate for the constant colour field of two opposite charges $Q-\bar{Q}$ to create a parton pair with the same colour charges $Q-\bar{Q}$ and transverse mass M_t for unit string length and time is taken by the Schwinger expression

$$W \sim K_{[N]}^2 \exp(-\pi M_t^2 / K_{[N]}) \quad , \quad (1)$$

where $K_{[N]}$ is the string tension for the $[N]$ $SU(3)$ representation proportional to the corresponding quadratic Casimir operator $C_{[N]}^2$. In our case

$$C_{[3]}^2 = 4/3, \quad C_{[6]}^2 = 10/3, \quad C_{[8]}^2 = 3 \quad . \quad (2)$$

The fragmentation of the fused strings produces more baryons and antibaryons, especially strange ones, than in the case of the fragmentation of the original strings. These enhancements are accompanied by a strong reduction of particle production in the central rapidity region.

3 Cumulative particle production

Particle production outside the nucleon–nucleon kinematical limits is a well known effect, called cumulative effect, studied both theoretically and experimentally ([22, 23, 24, 25, 26]). However at high enough energies, where the string picture can be applied, there are only data from one collaboration at 400 GeV/c ([26]), with incoming protons against nuclei: Li, Be, C, Al, Cu and Ta. We have generated 10000 events for each p–A collision in our Monte Carlo code. The results together with the experimental data for the invariant differential cross sections for production of protons, positive pions and positive kaons are shown in Tables 1 and 2.

If the invariant differential cross section is parametrized as a function of x_F in the exponential form:

$$\sigma \sim \exp(-bx) \tag{3}$$

the slope b is in the range 5–6 for all cases in agreement with the experimental data. If the fusion of strings is not included the obtained b value is in the range 10–11 quite far from the data.

The fusion of strings describes also rightly the dependence of the inclusive cross section with the kinetic energy. As an example, in Fig. 1, it is shown the experimental data for the positive pion inclusive cross section for p–Ta collisions together the results with and without fusion of strings.

The A–dependence of the cumulative effect is usually parametrized as $A^{\alpha(x)}$. The value of $\alpha(x)$ has been proposed ([24]) to be the function

$$\sigma \sim A^{\alpha(x)}, \quad \alpha(x) = 1 + 1/3 (x - 1). \tag{4}$$

which is plotted in Fig. 2 together the $\alpha(x)$ obtained from the experimental data which is very close to the above straight line. Also the $\alpha(x)$ obtained from the fusion of strings is close to the experimental data, indeed it fits into the line $\alpha(x) = 1 + 0.4(x - 1)$.

From all these comparisons we can conclude that a reasonable agreement for p–A cumulative particle spectrum is obtained. Notice that we do not have any free parameter. We could improve the comparison by introducing minor effects like rescattering or a more detailed nucleon and quark correlations (other than Fermi motion, which has already been included in our code). However our goal is not to obtain a perfect fit but just to check if the string fusion works reasonable well.

Once it has been checked that our model is consistent with the hadron–nucleus experimental data, we turn to nucleus–nucleus collisions, simulating 10000 central S–S collisions and 1000 central Pb–Pb collisions at $\sqrt{s} = 19.4$ AGeV. Also central Pb–Pb collisions at RHIC energies ($\sqrt{s} = 200$ AGeV) have been simulated. Distributions of baryons and mesons in central S–S collisions at SPS energies with x_F larger than 1 are shown in Fig. 3. In Fig. 4 the separated spectra of protons, neutrons, lambdas, K^0 , K^+ , K^- , π^0 , π^+ and π^- are presented. Fig. 5 and Fig. 6 show the same distributions for the case of central Pb–Pb collisions at $\sqrt{s} = 19.4$ AGeV. The results for Pb–Pb collisions at $\sqrt{s} = 200$ AGeV are very similar to the ones at $\sqrt{s} = 19.4$ AGeV. In 1000 events 2015 particles are found with $|x_F|$ larger than 1 to compare with 1783 at $\sqrt{s} = 19.4$ AGeV. This small change is due to a moderate increase of the number of strings with energy. In general, it is seen that many baryons and mesons are produced with x_F larger than 1.

4 String fusion at ultrahigh cosmic ray energies

String fusion produces a strong suppression of multiplicities. In the limit of a very strong fusion, the multiplicity in hadron–nucleus collisions turns out independent of A instead of $\sim A^{1/3}$. Also the squared dispersion D^2 behaves like $A^{-1/3}$ instead of $A^{1/3}$. At finite energies the fusion of strings is not strong and it is not expected such a behaviour,

however the reduction of multiplicities is quite sizable for heavy ion collisions at RHIC and LHC energies. For instance, simulations done for ALICE detector for LHC indicate that the multiplicity is a factor between 2.5 and 4 less than the one obtained in the models without fusion.

This suppression of multiplicities can explain the rise of the average shower depth of maximum in cosmic rays as the energy increases, without requiring any change in the chemical composition. It is usually accepted that there is a change in the cosmic ray chemical composition between 10^{16} eV and 10^{19} eV. It seems that the composition becomes significantly lighter with increasing energy, going from a heavy composition at 10^{16} eV to a light one at energies higher than 10^{19} eV. The distribution of the shower depth of maximum as a function of energy has been studied using a simple model of two components ([15]), observing that the composition of the primary changes from approximately 75 % of iron component and a 25 % of proton component at 10^{16} eV to 50 % of iron and a 50 % of proton at 10^{19} eV. To study this point, we have computed the multiplicities of p–Air and Fe–Air interactions with and without string fusion in the whole range of energies studied (from 10^{16} to 10^{19} eV). As it can be seen in Fig. 7, with string fusion the multiplicity for a constant composition of 10 % of proton and 90 % of iron in the whole range of energy, essentially reproduces the multiplicity obtained without string fusion for a uniform change in the composition from 75 % Fe and 25 % proton at 10^{16} eV to 50 % Fe and 50 % proton at 10^{19} eV. Thus the string fusion does the same job as the composition change.

Therefore, the change in the energy behaviour of the average shower depth of maximum X_{max} can be ascribed to a change in the interaction mechanism with the increasing role of collective effects like string fusion, and not to a change in the chemical composition of the primary cosmic rays. Further studies of this point would require combining the code used in this paper with the standard codes which describe the full cascade.

Work in this direction is in progress.

Once we know that it is reasonable to assume that most of the primary cosmic rays are iron nuclei, we would like to know how many particles are going to be accelerated due to the string fusion mechanism and get energy-momentum larger than the permitted limits in nucleon–nucleon collisions.

To study the case relevant for cosmic rays we simulated 1000 Fe–Air collisions at 10^{17} eV (we used this energy and not 10^{20} eV to save computing time, rendering the simulation reliable). In this sample 198 particles with $|x_F| > 1$ were found. The average number of strings was found to be 225, from which 62 joined to form double strings. As mentioned, our code only includes fusion of two strings. However we can estimate the number of strings participating in a triple fusion assuming that the probability for triple fusion is roughly the square of that for double fusion. Then one would expect that 18 strings join to form triple strings and 4 strings join to form a quadruple string. Other reasonable assumptions about the probability of triple fusion give similar results. Therefore the probability of obtaining particles with $|x_F| > 2$ or even $|x_F| > 3$ does not seem to be negligible. Triggering central collisions, particles with $|x_F| > 4$ could even be detected. The energy around $3 \cdot 10^{20}$ eV measured in several cosmic ray experiments could then be lowered by a factor 2 to 4 if the described effect is present and there are particles in the shower with $|x_F| > 2$ or $|x_F| > 3$. This lower energy for the primary may lie below the energy cut-off due to the scattering of cosmic rays on the microwave background. Indeed, according to the computation of F. W. Stecker ([19]) the attenuation mean free path increases more than one order of magnitude. This fact means that the measured energies are compatible with the effective cut-off.

5 Conclusions

The string fusion mechanism produces particles with more energy–momentum than the original nucleon–nucleon collisions. In this way it can be considered as a hadronic accelerator. We have shown that string fusion reproduces reasonably well the experimental data on cumulative effect in proton–nucleus collisions giving a sizable number of protons, neutrons, lambdas and pions in central nucleus–nucleus collisions already at $\sqrt{s} = 19.4$ AGeV. The experimental confirmation of this at SPS will be welcome.

Concerning cosmic rays, string fusion can explain the reduction of multiplicities in the energy range between 10^{16} eV and 10^{19} eV without requiring a change in the chemical composition. Also, string fusion provides a natural hadronic accelerator to reach energies above 10^{20} eV without requiring any additional unusual cosmic accelerator. Our predictions can be checked in future heavy ion experiments at the accelerators RHIC, LHC and also in cosmic ray experiments (concretely the Auger proyect ([27])).

In conclusion we would like to thank N. S. Amelin, A. Capella, J. W. Cronin, G. Parente, J. Ranft and E. Zas for useful comments and discussions and the Comisión Interministerial de Ciencia y Tecnología (CICYT) of Spain for financial support. M. A. Braun thanks IBERDROLA, E. G. Ferreiro thanks Xunta de Galicia and Yu. M. Shabelski the Dirección General de Política Científica of Spain for financial support. This work was partially supported by the INTAS grant N 93–0079.

References

- [1] B. Andersson, G. Gustafson and B. Nilsson–Almqvist, Nucl. Phys. **B281** (1987) 289; M. Gyulassy, CERN preprint CERN–TH 4794 (1987).

- [2] A. Capella, U. P. Sukhatme, C.-I. Tan and J. Tran Thanh Van, Phys. Rep. **236** (1994) 225.
- [3] K. Werner, Phys. Rep. **232** (1993) 87.
- [4] H. Sorge, H. Stöcker and W. Greiner, Nucl. Phys. **A498** (1989) 567c.
- [5] C. Pajares, Proceedings of the International Workshop on Quark Gluon Signatures, Strasbourg, France, October 1–4 1990; M. A. Braun and C. Pajares, Phys. Lett. **B287** (1992) 154; Nucl. Phys. **B390** (1993) 559; Nucl. Phys. **B390** (1993) 542.
- [6] B. Andersson and P. Henning, Nucl. Phys. **B355** (1991) 82.
- [7] H. Sorge, M. Berenguer, H. Stöcker and W. Greiner, Phys. Lett. **B289** (1992) 6.
- [8] H.-J. Möhring, J. Ranft, C. Merino and C. Pajares, Phys. Rev. **D47** (1993) 4142; C. Merino, C. Pajares and J. Ranft, Phys. Lett. **B276** (1992) 168.
- [9] K. Werner and J. Aichelin, Phys. Lett. **B308** (1993) 372.
- [10] J. Ranft, A. Capella and J. Tran Thanh Van, Phys. Lett. **B320** (1994) 346.
- [11] N. S. Amelin, M. A. Braun and C. Pajares, Phys. Lett. **B306** (1993) 312; Z. Phys. **C63** (1994) 507.
- [12] N. Armesto, M. A. Braun, E. G. Ferreira and C. Pajares, Phys. Lett. **B344** (1994) 301.
- [13] N. S. Amelin, N. Armesto, M. A. Braun, E. G. Ferreira and C. Pajares, Phys. Rev. Lett. **73** (1994) 2013.
- [14] D. J. Bird *et al.*, Phys. Rev. Lett. **21** (1993) 3401; Astrophys. J. **42** (1994) 491.

- [15] T. K. Gaisser *et al.*, Phys. Rev. **D47** (1993) 1919.
- [16] N. N. Efimov *et al.*, Proceedings of the International Workshop on Astrophysical Aspects of the Energetic Cosmic Rays, Kofú 1990.
- [17] N. Hayshida *et al.*, Phys. Rev. Lett. **73** (1994) 3491; S. Yoshida *et al.*, Astropart. Phys. **3** (1995) 105.
- [18] K. Greisen, Phys. Rev. Lett. **16** (1966) 748; G. T. Zatsepin and V. A. Kuzmin, JETP Lett. **4** (1966) 78.
- [19] F. W. Stecker, Phys. Rev. Lett. **21** (1968) 1016.
- [20] G. Sigl, S. Lee, D. N. Schramm and P. Bhattacharjee, Univ. Chicago preprint (1996).
- [21] J. Engel, T. K. Gaisser, P. Lipari and T. Stanev, Phys. Rev. **D46** (1991) 5013.
- [22] A. M. Baldin *et al.*, Yad. Fiz. **20** (1974) 1210; Sov. J. Nucl. Phys. **20** (1975) 629.
- [23] M. I. Strikman and L. L., Frankfurt Phys. Rep. **76** (1981) 215.
- [24] A. V. Efremov, A. B. Kaidalov, V. T. Kim, G. I. Lykasov and N. V. Slavin, Sov. J. Nucl. Phys. **47** (1988) 868.
- [25] M. A. Braun and V. Vechermin, Nucl. Phys. **B427** (1994) 614.
- [26] Y. D. Bayukov *et al.*, Phys. Rev **C20** (1979) 764, Phys. Rev. **C22** (1980) 700.
- [27] The Pierre Auger Project, Design Report, October 1995.

Table captions

Table 1. Comparison of experimental data ([26]) on the invariant differential cross section $\sigma = E \frac{d\sigma}{dp_3}$ (GeV mb/(GeV/c)³ sr nucleon) for π^+ and K^+ vs p (GeV/c), laboratory angle 118° , $P_{lab} = 400$ GeV, for p–Li and p–Ta collisions with the String Fusion Model code results, with and without string fusion.

Table 2. Comparison of experimental data ([26]) on the invariant differential cross section $\sigma = E \frac{d\sigma}{dp_3}$ (GeV mb/(GeV/c)³ sr nucleon) for π^+ vs p (GeV/c), laboratory angle 118° , $P_{lab} = 400$ GeV, for p–Li and p–Ta collisions with the String Fusion Model code results, with and without string fusion.

Figure captions

Fig. 1. Comparison of experimental data ([26]) (continuous line) on the invariant differential cross section $\sigma = E \frac{d\sigma}{dp_3}$ for π^+ vs kinetic energy (GeV), laboratory angle 118° , $P_{lab} = 400$ GeV, for p-Ta collisions with the String Fusion Model code results, with (upper dashed line) and without string fusion.

Fig. 2. α vs x . $\alpha = 1 + 1/3 (x - 1)$ (continuous line), experimental result (nearer dashed line) and our results with fusion.

Fig. 3. x_F distributions for $x_F > 1$ in S-S collisions (10000 events) at $\sqrt{s} = 19.4$ AGeV of mesons (a) and baryons (b) with (continuous line) and without (dashed line) string fusion. No mesons are found in the no fusion case.

Fig. 4. x_F distributions for $x_F > 1$ in S-S collisions (10000 events) at $\sqrt{s} = 19.4$ AGeV of protons (a), neutrons (b), lambdas (c), K^0 (d), K^+ (e), K^- (f), π^0 (g), π^+ (h) and π^- (i) with (continuous line) and without (dashed line) string fusion. No mesons are found in the no fusion case.

Fig. 5. x_F distributions for $x_F > 1$ in Pb-Pb collisions (1000 events) at $\sqrt{s} = 19.4$ AGeV of mesons (a) and baryons (b) with (continuous line) and without (dashed line) string fusion. No mesons are found in the no fusion case.

Fig. 6. x_F distributions for $x_F > 1$ in Pb-Pb collisions (1000 events) at $\sqrt{s} = 19.4$ AGeV of protons (a), neutrons (b), lambdas (c), K^0 (d), K^+ (e), K^- (f), π^0 (g), π^+ (h) and π^- (i) with (continuous line) and without (dashed line) string fusion. No mesons are found in the no fusion case.

Fig. 7. Total multiplicity dependence on the primary energy for a fixed composition $\langle n_t \rangle = 0.1 \langle n_{p-Air} \rangle + 0.9 \langle n_{Fe-Air} \rangle$ in the fusion case and a uniform change in the composition from $\langle n_t \rangle = 0.25 \langle n_{p-Air} \rangle + 0.75 \langle n_{Fe-Air} \rangle$ at 10^{16} eV to $\langle n_t \rangle = 0.5 \langle n_{p-Air} \rangle + 0.5 \langle n_{Fe-Air} \rangle$ at 10^{19} eV in the no fusion case (dashed

line).

Table 1

Reaction	$p - Li$	$p - Li$	$p - Li$
p momentum	Experiment	Without fusion	With fusion
	σ for π^+	σ for π^+	σ for π^+
0.200	5.75 ± 0.79	3.53	4.77
0.293	1.89 ± 0.26	0.314	1.41
0.381	0.672 ± 0.046	0.07	0.38
0.474	0.217 ± 0.016	0	0.34
0.580	$(0.509 \pm 0.044)10^{-1}$	0	0.094
0.681	$(0.128 \pm 0.012)10^{-1}$	0	0.009
Reaction	$p - Ta$	$p - Ta$	$p - Ta$
p momentum	Experiment	Without fusion	With fusion
	σ for π^+	σ for π^+	σ for π^+
0.200	8.57 ± 1.14	5.65	6.60
0.293	2.20 ± 0.31	0.19	1.57
0.394	0.78 ± 0.068	0.038	0.38
0.489	0.309 ± 0.032	0.032	0.173
0.583	0.135 ± 0.017	0	0.072
0.680	$(0.386 \pm 0.076)10^{-1}$	0	0.038
	σ for K^+	σ for K^+	σ for K^+
0.539	$(0.241 \pm 0.100)10^{-1}$	0	0.037
0.584	$(0.372 \pm 0.763)10^{-2}$	0	0

Table 2

Reaction	$p - Li$	$p - Li$	$p - Li$
p momentum	Experiment	Without fusion	With fusion
	σ for protons	σ for protons	σ for protons
0.385	4.17 ± 0.23	1.24	2.82
0.476	1.76 ± 0.11	0	1.01
0.581	0.61 ± 0.04	0	0.47

Reaction	$p - Ta$	$p - Ta$	$p - Ta$
p momentum	Experiment	Without fusion	With fusion
	σ for protons	σ for protons	σ for protons
0.395	29.9 ± 1.5	15.1	22.3
0.490	13.2 ± 0.7	0	12.57
0.585	5.2 ± 0.3	0	2.5

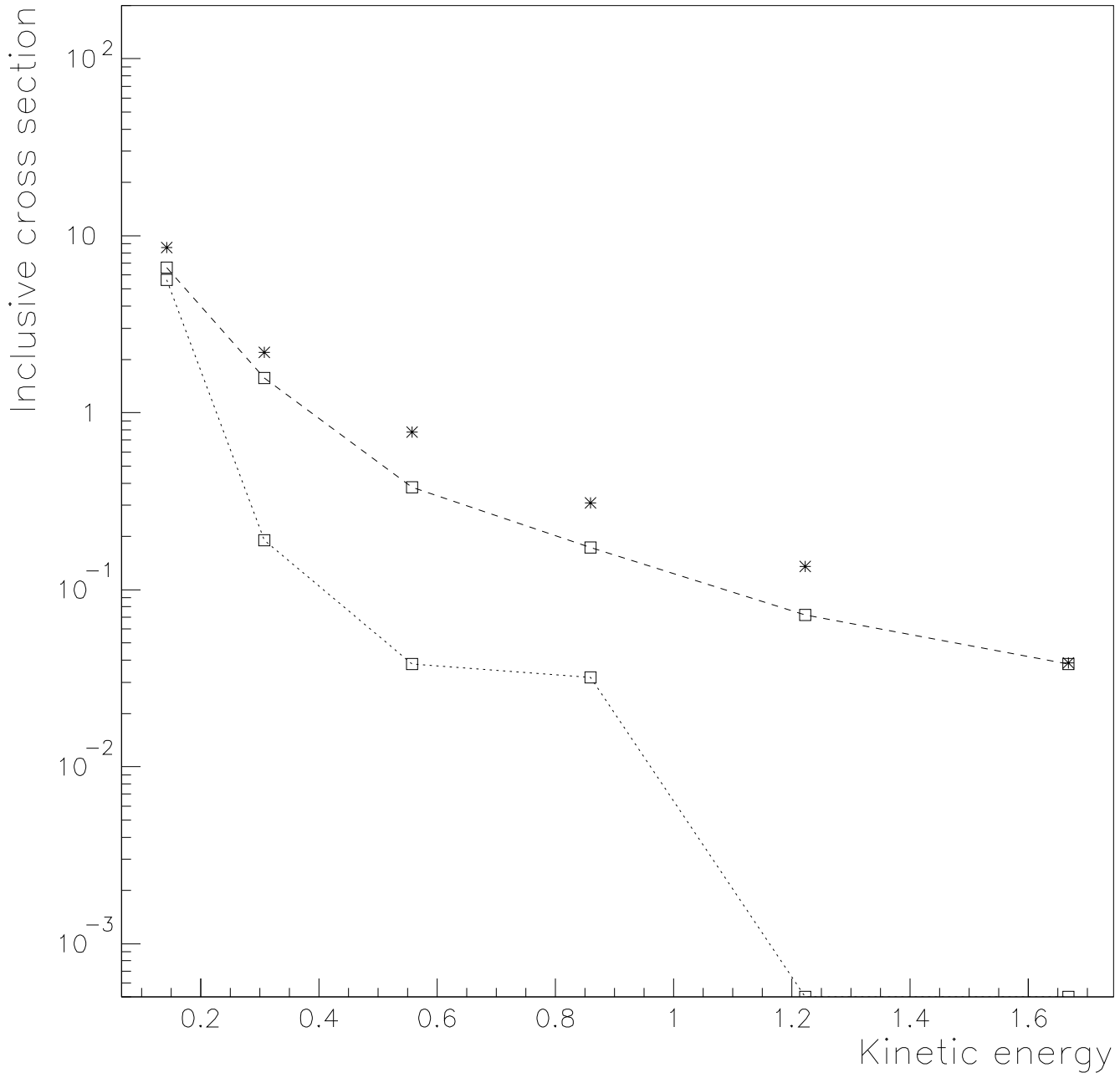


Fig. 1

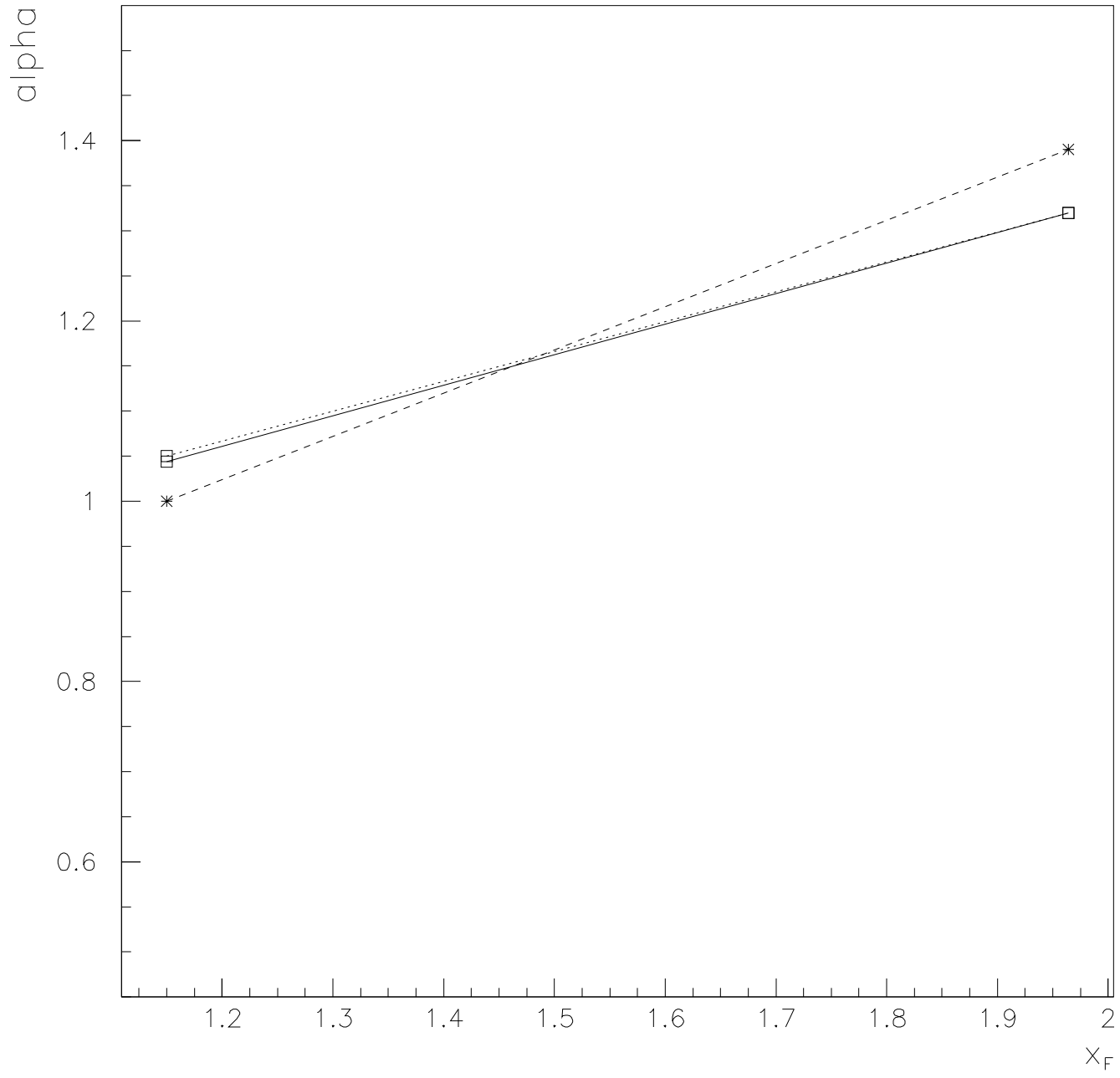


Fig. 2

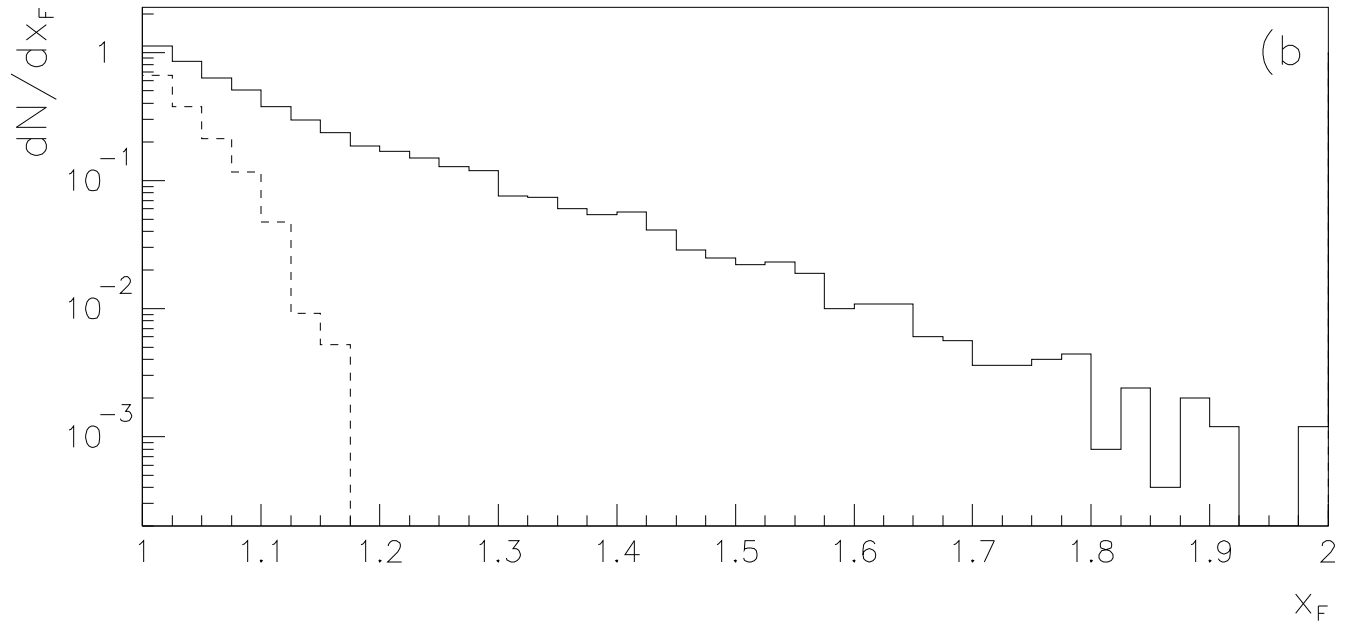
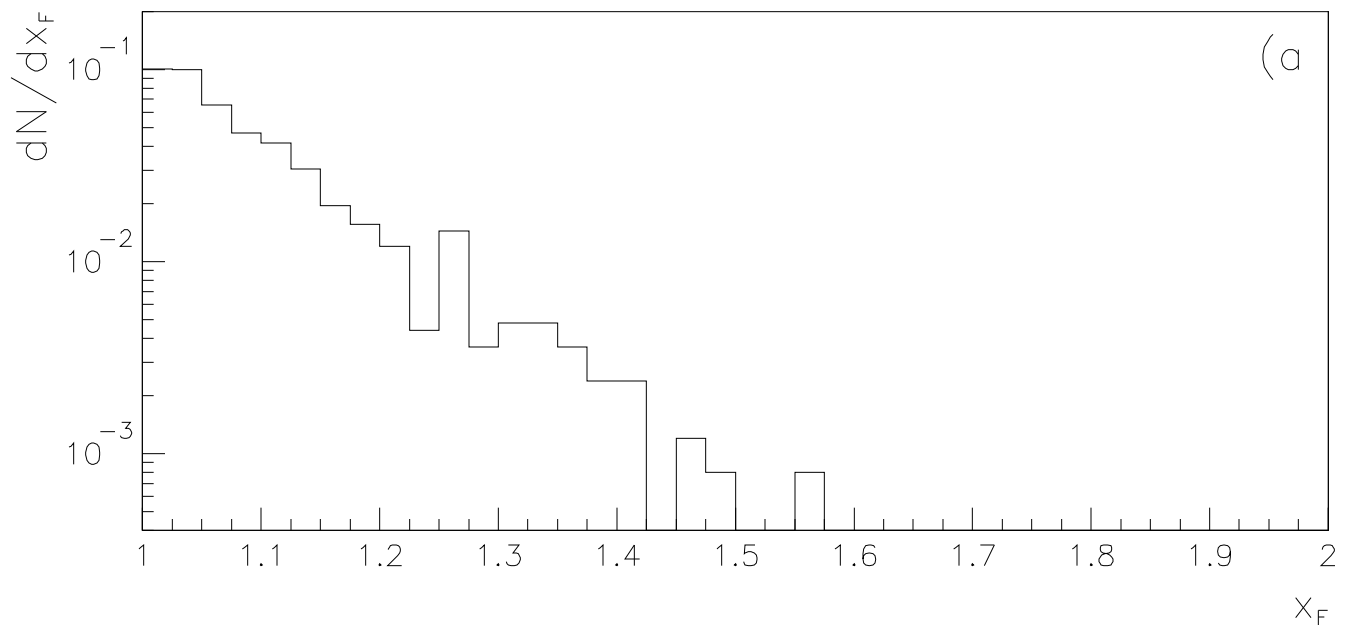


Fig. 3

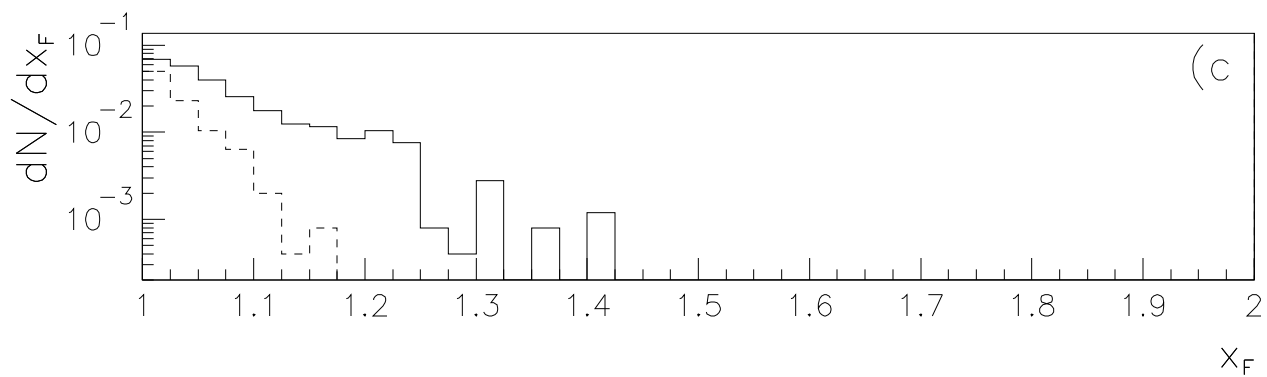
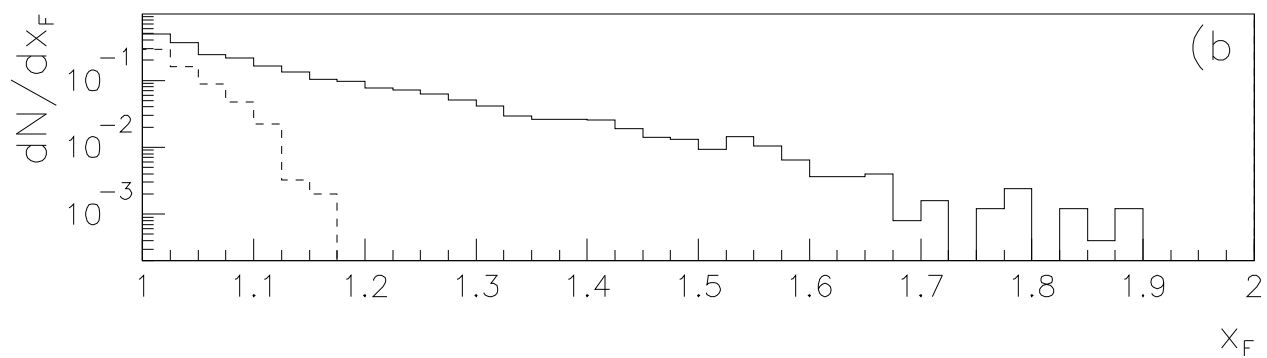
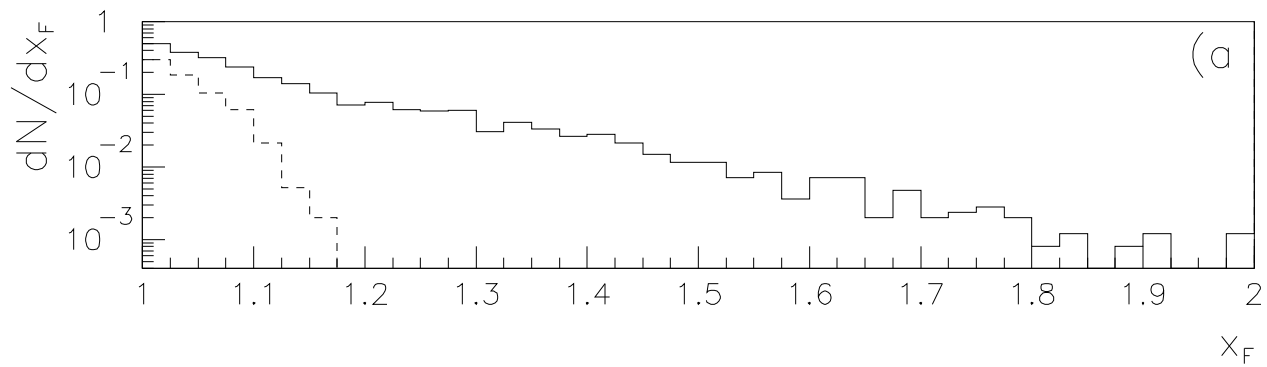


Fig. 4

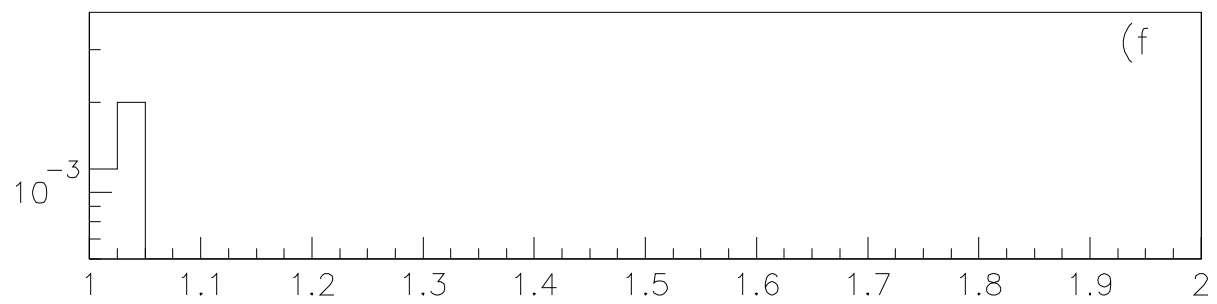
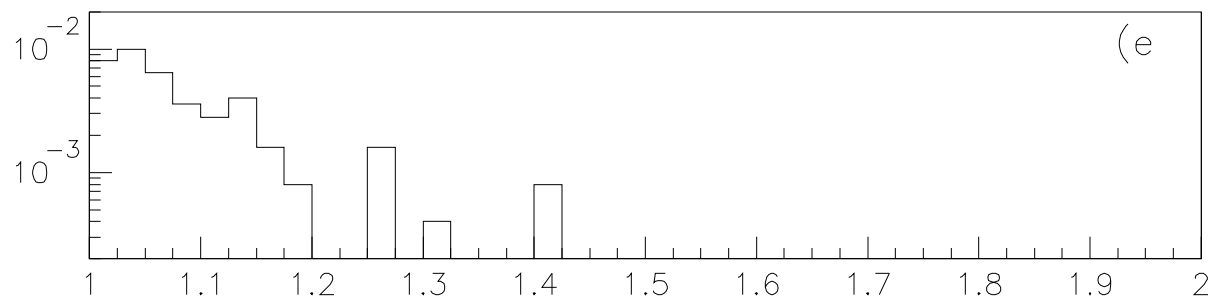
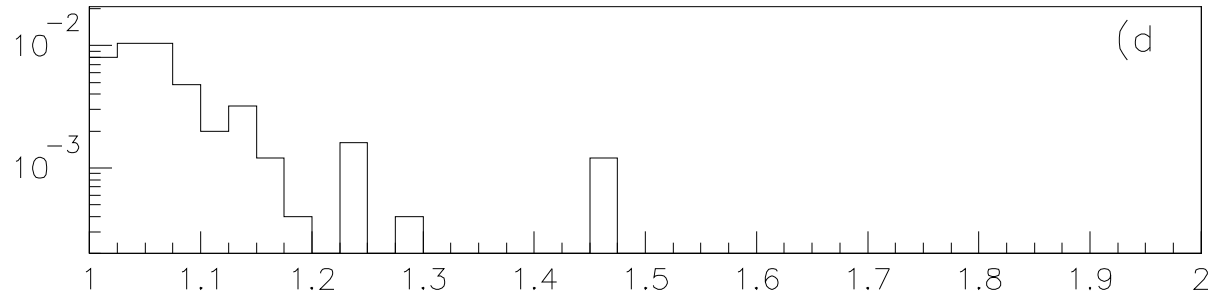


Fig. 4

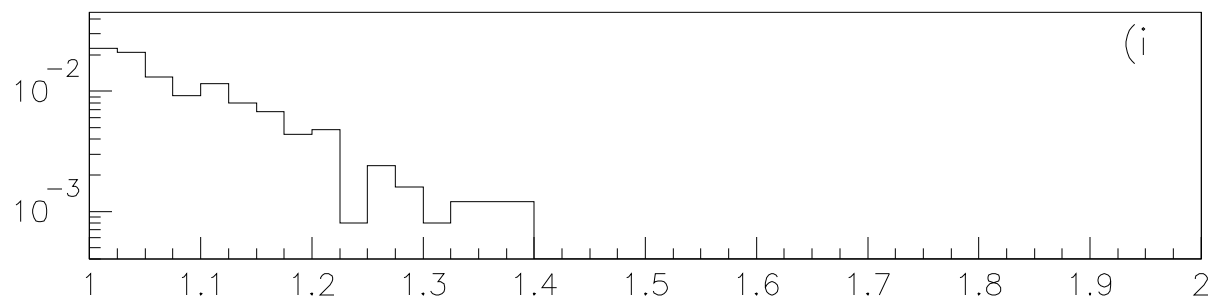
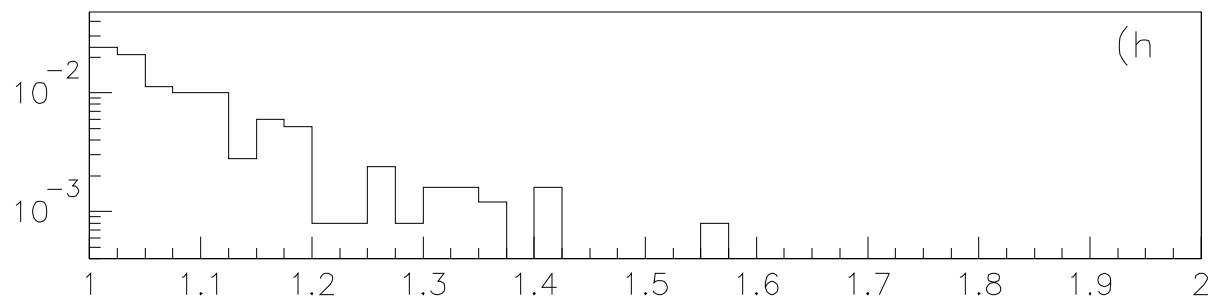
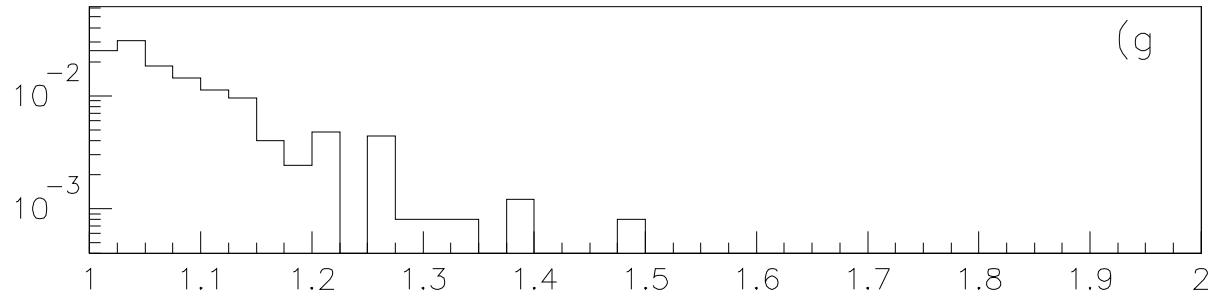


Fig. 4

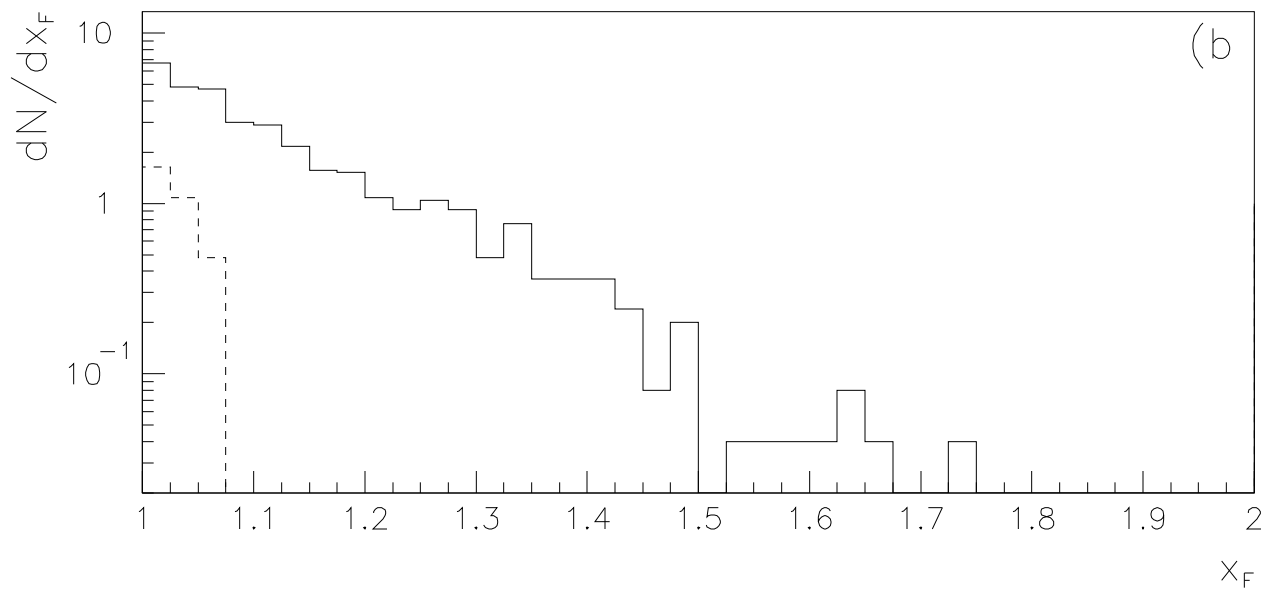
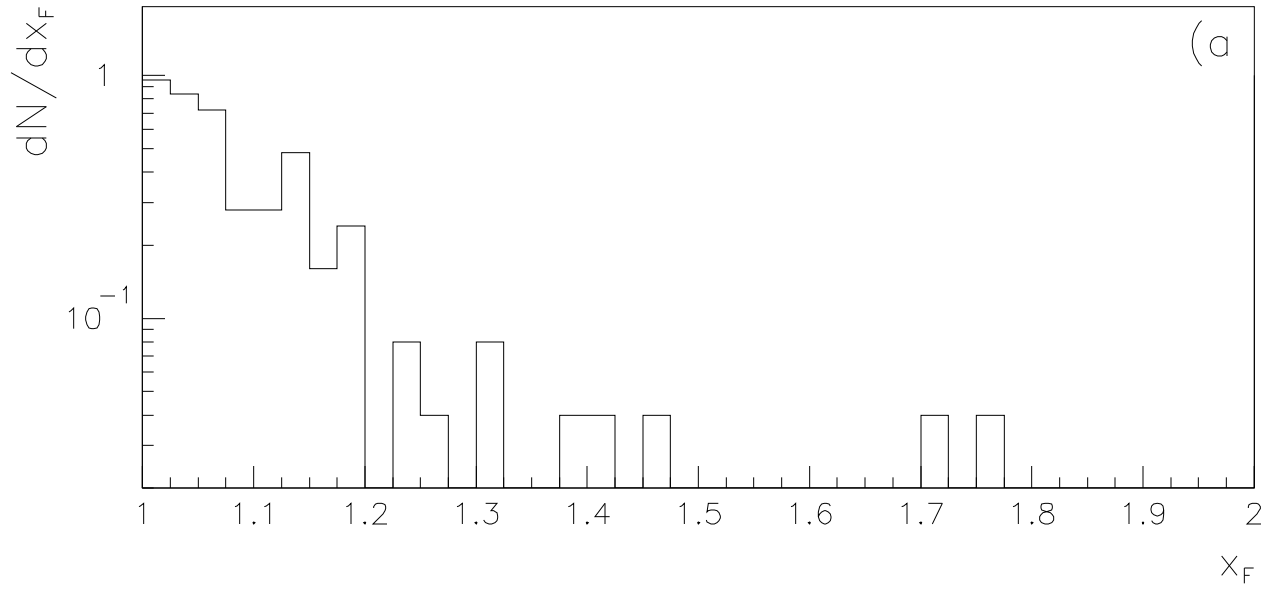


Fig. 5

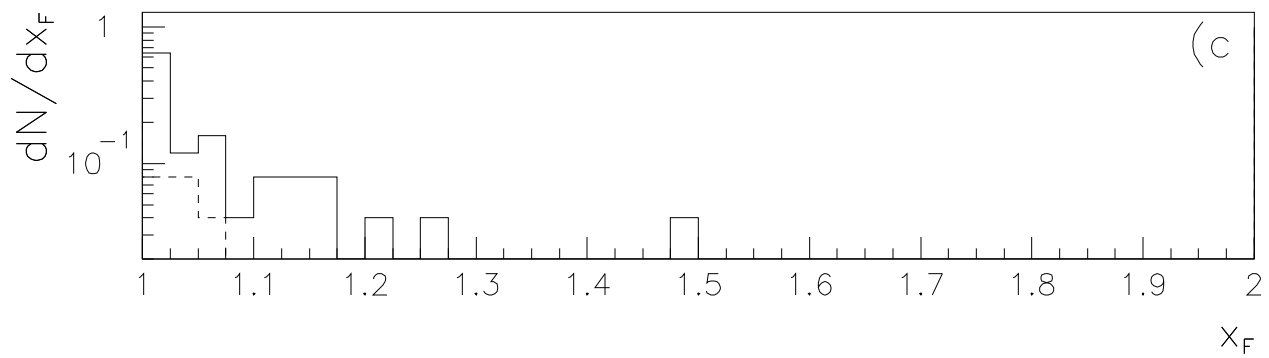
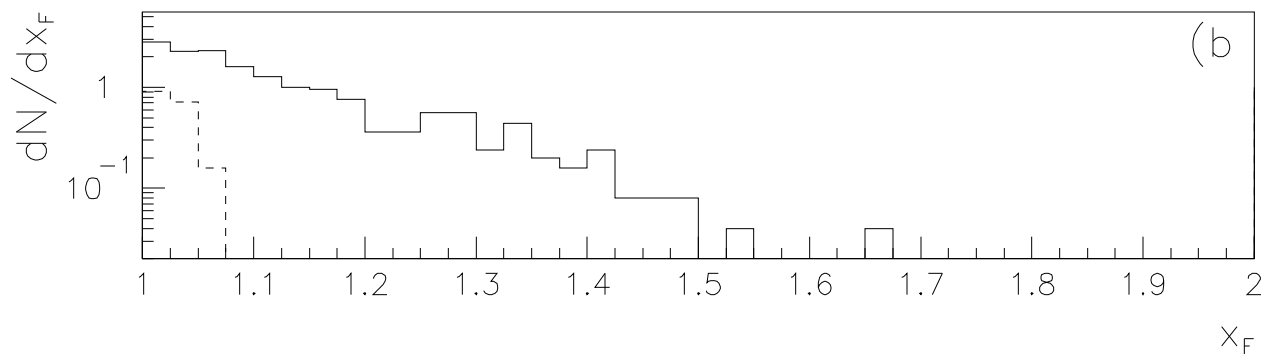
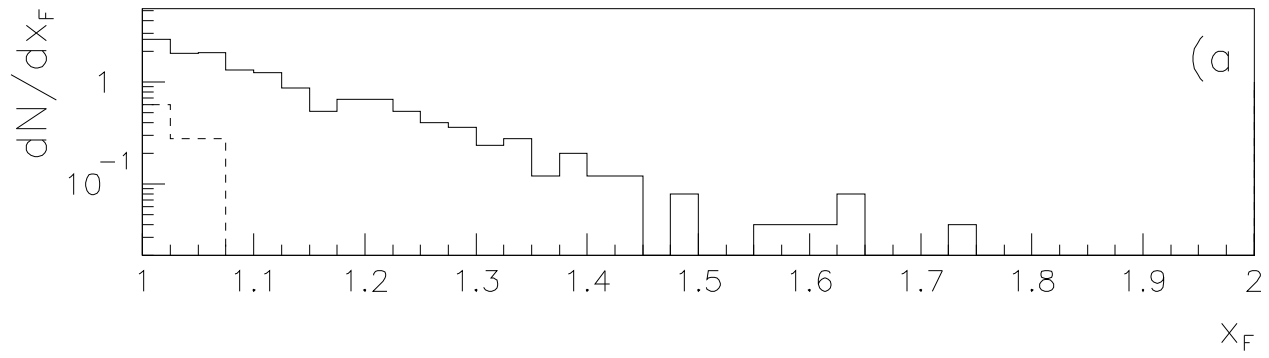


Fig. 6

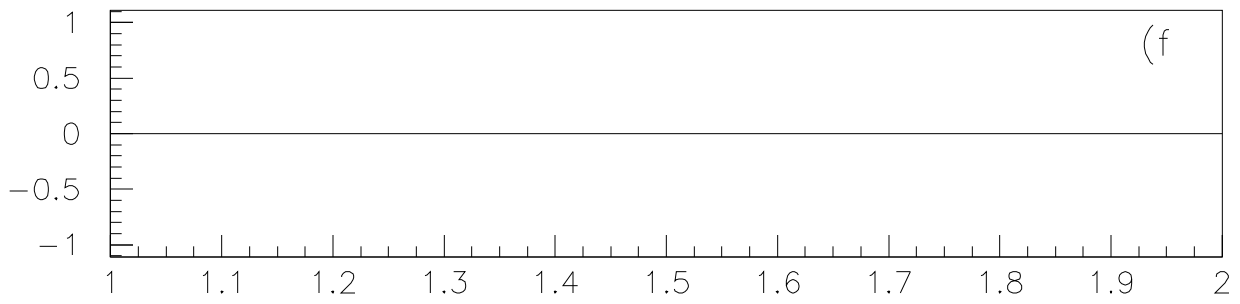
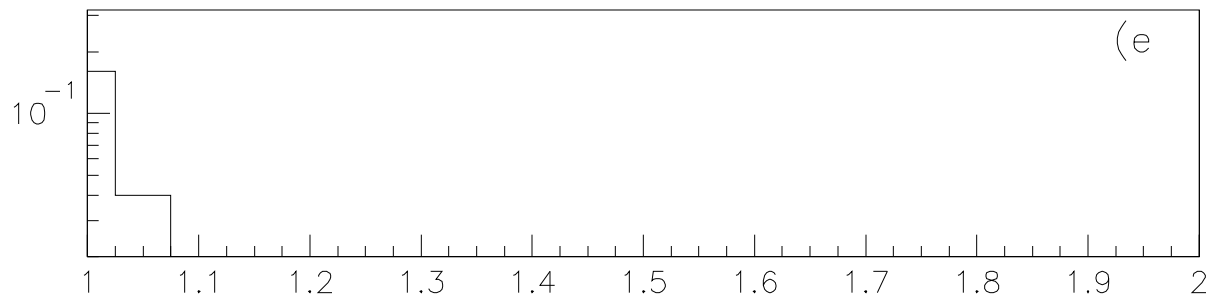
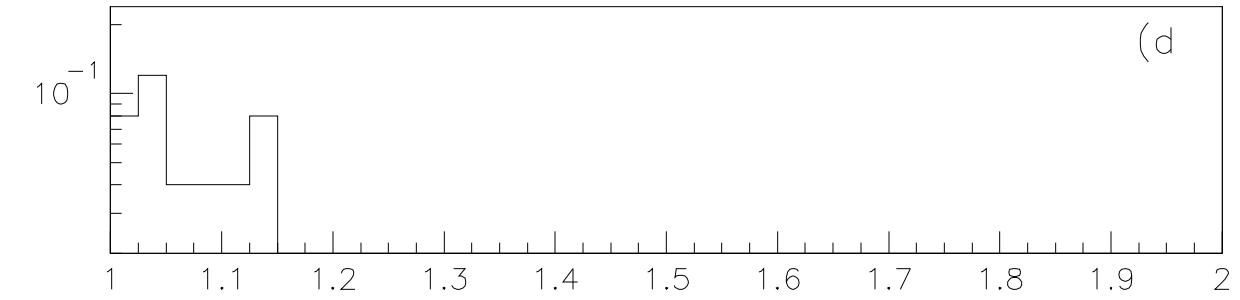


Fig. 6

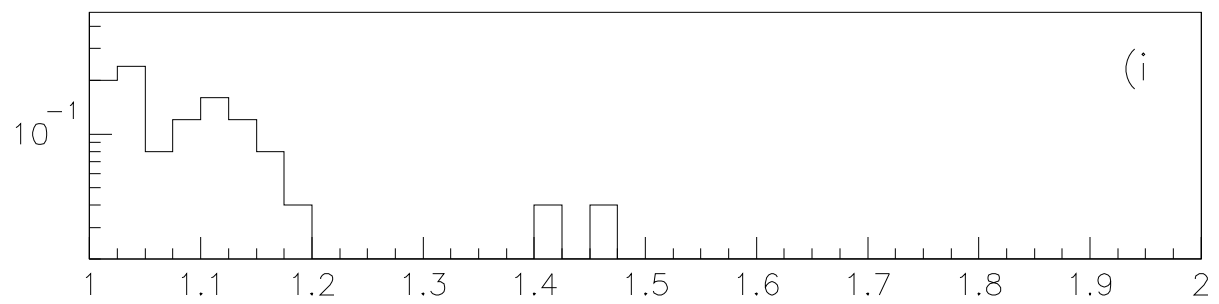
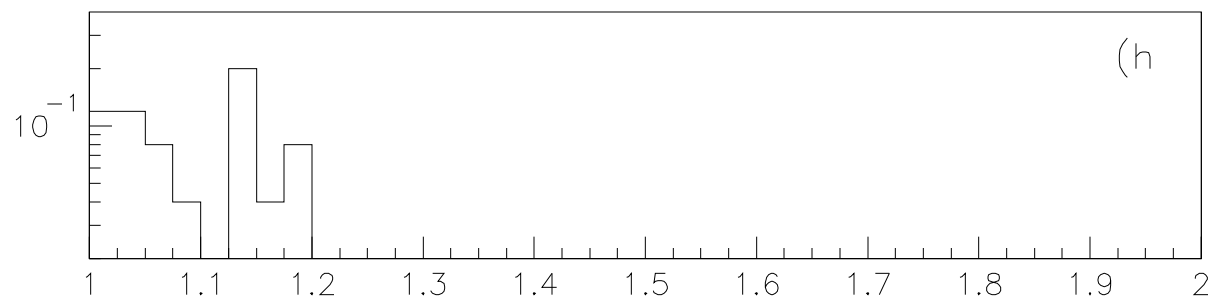
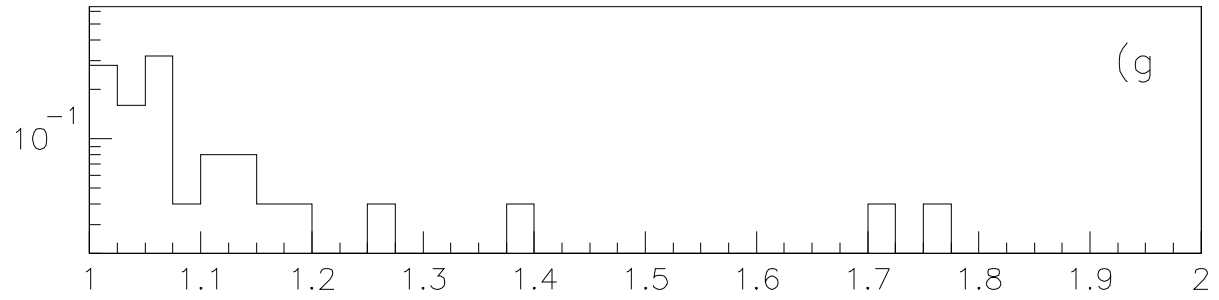


Fig. 6

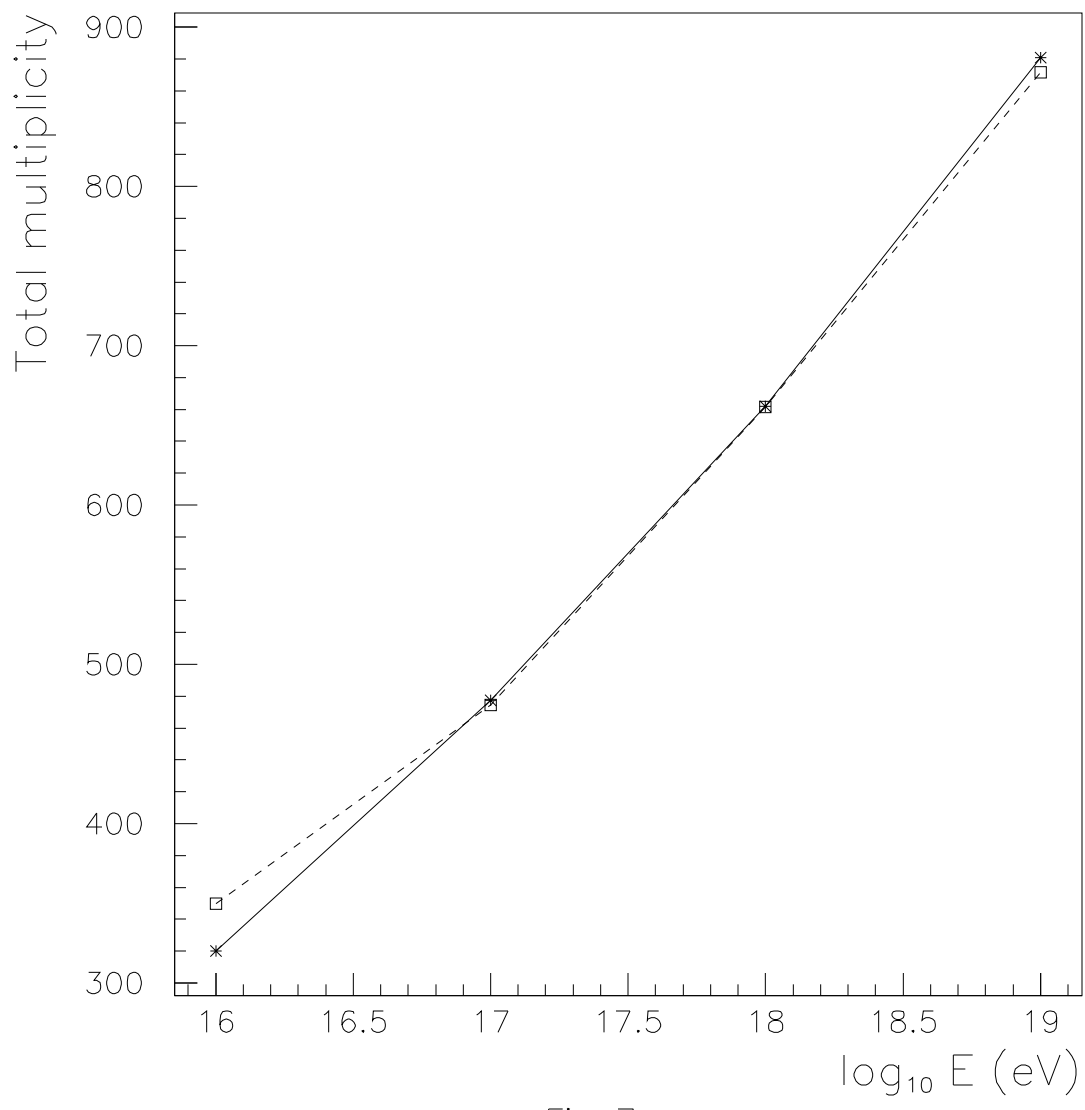


Fig. 7